

# AN NEW POLAR FACTOR RETRACTION ON THE STIEFEL MANIFOLD WITH CLOSED-FORM INVERSE\*

RASMUS JENSEN<sup>†</sup> AND RALF ZIMMERMANN<sup>†</sup>

**Abstract.** Retractions are the workhorse in Riemannian computing applications, where computational efficiency is of the essence. This work introduces a new retraction on the compact Stiefel manifold of orthogonal frames. The retraction is second-order accurate under the Euclidean metric and features a closed-form inverse that can be efficiently computed. To the best of our knowledge, this is the first Stiefel retraction with both these properties. A variety of retractions is known on the Stiefel manifold, including the Riemannian exponential map, the polar factor retraction, the QR-retraction and the Cayley retraction, but none of them features a closed-form inverse. The only Stiefel retraction with closed-form inverse that we are aware of is based on quasi-geodesics, but this one is of first order.

**Key words.** Stiefel manifold, retraction, manifold interpolation, manifold optimization, local coordinates, Riemannian exponential, geodesics, Riemannian computing

**MSC codes.** 15A16, 15B10, 53Z50, 65D05, 65F60

**1. Introduction.** Practical data processing on manifolds requires local coordinates, which make it possible to map data ‘there and back’: ‘There’ means mapping data from a Euclidean coordinate domain, for example on the tangent space, to the manifold. ‘Back’ refers to the reverse action of mapping manifold data into a coordinate domain. In certain applications, e.g., Riemannian optimization, only the ‘there’-direction is needed, but for manifold interpolation or for computing Riemannian averages, there must also be an efficient way to go ‘back’.

While the Riemannian normal coordinates, i.e., the Riemannian exponential and logarithm maps, enjoy desirable geometric features and are often best-suited for theoretical analysis, their first-order approximations, called retraction maps, are the workhorse in applications where computational efficiency is of the essence. By definition, all retractions are local diffeomorphisms.

This work focuses on the Stiefel manifold of orthogonal frames. Popularized by [3], the Stiefel manifold features in a huge amount of applications in deep learning, computer vision, signal processing, medical imaging and general numerical linear algebra, and the associated literature is ever growing.

Various retractions are known on the Stiefel manifold. We are aware of the following:

- (1) the Riemannian exponential map [3],
- (2) the polar factor retraction [1, Section 4],
- (3) the QR retraction [1, Section 4],
- (4) the Cholesky QR-based retraction [13],
- (5) the Cayley retraction [15].
- (6) the quasi-geodesic retractions of [2].

The Riemannian exponential (1) is the reference when quantifying the retraction order. Computing the inverse requires an iterative algorithm [16, 14, 11]. The polar factor retraction (2) is of second order under the Euclidean metric. The QR-retraction (3) is of first order and so is its Cholesky counterpart (4). Computing the inverse

---

\*Submitted to the editors DATE.

**Funding:** This work was supported by the Independent Research Foundation Denmark, DFF, grant nr. 3103-00094B

<sup>†</sup>Department of Mathematics and Computer Science, SDU Odense (rasmusj@imada.sdu.dk, zimmermann@imada.sdu.dk).

maps for the retractions (2) and (3) is based on solving a Sylvester/Riccati/Lyapunov-type matrix equation [10]. For the Cholesky QR-based retraction and the Cayley retraction, we are not aware of any published work on computing the inverse, but as with (2), (3) a matrix equation is expected to arise in the task. To the best of our knowledge, the quasi-geodesic retractions of (6) are the only ones on the list that feature a closed form inverse. The retraction order is 1.

In this work, we introduce a new retraction on the Stiefel manifold that is based on an additional twist (quite literally) in the polar factor retraction. The main features of this retraction, which we call *polar-light retraction*, are:

- It is second-order accurate under the Euclidean metric.
- It has a closed-form inverse.
- Evaluating its inverse incurs essentially the same computational cost as evaluating the retraction itself. Computing matrix functions and decompositions is necessary only for small ( $p \times p$ ) matrices; with large ( $n \times p$ ) matrices, only simple matrix–matrix multiplications arise.

**2. Background.** The orthogonal group and special orthogonal group are

$$O(n) = \{\mathbf{Q} \in \mathbb{R}^{n \times n} \mid \mathbf{Q}^T \mathbf{Q} = I_n\}, \text{ and } SO(n) = \{\mathbf{Q} \in O(n) \mid \det(\mathbf{Q}) = 1\}.$$

The Stiefel manifold is their rectangular relative

$$\text{St}(n, p) = \{U \in \mathbb{R}^{n \times p} \mid U^T U = I_p\}.$$

Here and throughout, we write  $I_p$  for the  $(p \times p)$ -identity matrix. We single out the special Stiefel point

$$E := \begin{bmatrix} I_p \\ 0 \end{bmatrix} \in \text{St}(n, p).$$

The dimension of the Stiefel manifold is  $\frac{p}{2}(p-1) + (n-p)p$ , which reflects the number of independent parameters in a skew-symmetric  $(p \times p)$ -matrix and a rectangular  $((n-p) \times p)$ -matrix. Fix  $\hat{U} \in \text{St}(n, p)$  with orthogonal completion  $\hat{U}_\perp \in \text{St}(n, n-p)$  so that  $\hat{\mathbf{Q}} = [\hat{U} \quad \hat{U}_\perp] \in O(n)$ . The tangent space at  $\hat{U}$  is

$$T_{\hat{U}} \text{St}(n, p) = \{\xi = \hat{\mathbf{Q}} \begin{bmatrix} A \\ B \end{bmatrix} \mid A \in \text{skew}(p), B \in \mathbb{R}^{(n-p) \times p}\} = \hat{\mathbf{Q}} T_E \text{St}(n, p).$$

For details, see [3, 1]. We denote the set of symmetric positive definite  $(p \times p)$ -matrices by  $\text{SPD}(p)$ .

**2.1. The classical Stiefel polar factor retraction.** With the help of the polar decomposition, any rectangular real matrix  $V \in \mathbb{R}^{n \times p}$  with full rank can be expressed as the unique product of the symmetric positive definite matrix square root  $S = \sqrt{V^T V}$  and the column-orthogonal –hence Stiefel– matrix  $U = VS^{-1}$ ,

$$V = US, \quad U \in \text{St}(n, p), \quad S \in \text{SPD}(p),$$

[7, Theorem 8.1]. It gives rise to the *polar factor retraction*:

$$(2.1) \quad R_{\hat{U}} : T_{\hat{U}} \text{St}(n, p) \rightarrow \text{St}(n, p), \xi = \hat{\mathbf{Q}} \begin{bmatrix} A \\ B \end{bmatrix} \mapsto (\hat{U} + \xi) (I_p + A^T A + B^T B)^{-\frac{1}{2}},$$

see [1, eq. (4.7)]. Note that  $\hat{U} + \xi = \hat{\mathbf{Q}}(E + [\frac{A}{B}])$  so that

$$(\hat{U} + \xi)^T (\hat{U} + \xi) = I_p + A^T A + B^T B = I_p + \xi^T \xi.$$

Hence,  $R_{\hat{U}}$  sends the (non-orthogonal)  $(n \times p)$ -matrix  $\hat{U} + \xi$  to the Stiefel manifold by mapping it to the orthogonal factor of its full polar decomposition. For the sake of argument, we call it the *full polar factor retraction*. Inversion requires solving a Lyapunov equation [10]. Higher-order extensions are discussed in [4].

**3. The polar-light retraction.** Any Stiefel matrix can be split into sub-blocks  $U = \begin{bmatrix} U_1 \\ U_2 \end{bmatrix}$  with  $U_1 \in \mathbb{R}^{p \times p}$  and  $U_2 \in \mathbb{R}^{(n-p) \times p}$ . A local coordinate representation can be obtained from a polar decomposition of the small block  $U_1$  alone; hence the term ‘light’.

LEMMA 3.1. *Consider the special point  $E = \begin{bmatrix} I_p \\ 0 \end{bmatrix} \in \text{St}(n, p)$ . The map*

$$\Psi_E : \text{St}(n, p) \supset \mathcal{B} \rightarrow T_E \text{St}(n, p) \cong \text{skew}(p) \times \mathbb{R}^{(n-p) \times p} \cong \mathbb{R}^{\frac{p}{2}(p-1) + (n-p)p}$$

$$U = \begin{bmatrix} U_1 \\ U_2 \end{bmatrix} \mapsto \begin{bmatrix} \log_m \left( U_1 (U_1^T U_1)^{-\frac{1}{2}} \right) \\ U_2 (U_1^T U_1)^{-\frac{1}{2}} \end{bmatrix} =: \begin{bmatrix} A \\ B \end{bmatrix}$$

is a coordinate chart on a (relative) open, path-connected neighborhood  $\mathcal{B} \subset \text{St}(n, p)$  around  $E$ .

Below, we state the inverse map  $\Psi_E^{-1}$ , which implicitly proves the lemma.

The chart  $\Psi_E$  can be interpreted as follows: A polar decomposition of the upper  $(p \times p)$ -block of  $U$  yields a splitting

$$U_1 = \underbrace{U_1 (U_1^T U_1)^{-\frac{1}{2}}}_{=: R \in O(p)} \underbrace{(U_1^T U_1)^{\frac{1}{2}}}_{=: S \in \text{SPD}(p)}.$$

Because there is a continuous path from  $E$  to  $U$ , and thus from the upper block  $I_p$  to the upper block  $U_1$ , it holds  $\det(R) = \det(U_1 (U_1^T U_1)^{-\frac{1}{2}}) = +1$ , so that  $R \in SO(p)$ . The following restrictions of the matrix exponential

$$\exp_m|_{\text{sym}(p)} : \text{sym}(p) \rightarrow \text{SPD}(p), \quad \exp_m|_{\text{skew}(p)} : \text{skew}(p) \rightarrow SO(p)$$

constitute a global diffeomorphism [12, Thm. 2.8] and a globally surjective local diffeomorphism [5, §. 3.11, Thm. 9], respectively. Hence, there is  $A \in \text{skew}(p)$  and  $X \in \text{sym}(p)$  such that  $R = \exp_m(A)$  and  $S = \exp_m(X)$  and

$$U_1 = RS = \exp_m(A) \exp_m(X).^1$$

Therefore,  $\Psi_E$  maps a Stiefel point  $\begin{bmatrix} U_1 \\ U_2 \end{bmatrix}$  from a suitable neighborhood of  $E$  to the components

$$A = \log_m(R), \quad B = U_2 \exp_m(X)^{-1}.$$

LEMMA 3.2. *The map  $\Psi_E$  is invertible; the inverse map  $\varphi_E = \Psi_E^{-1}$  is a local parameterization and is given by*

$$(3.1) \quad \varphi_E : \text{skew}(p) \times \mathbb{R}^{(n-p) \times p} \rightarrow \text{St}(n, p),$$

$$\begin{bmatrix} A \\ B \end{bmatrix} \mapsto \begin{pmatrix} \exp_m(A) \\ B \end{pmatrix} (I_{p \times p} + B^T B)^{-\frac{1}{2}}.$$

<sup>1</sup>This splitting represents the  $p^2$  degrees of freedom of a full-rank  $(p \times p)$ -matrix into  $\frac{1}{2}p(p-1)$  parameters for the skew-symmetric part and  $\frac{1}{2}p(p+1)$  parameters for the symmetric part in multiplicative form.

*Proof.* Recalling that the subblocks of a Stiefel matrix  $U$  are related by  $I_p = U_1^T U_1 + U_2^T U_2$ , it is straightforward to check the identities

$$\Psi_E \circ \varphi_E = \text{id}_{\text{skew}(p) \times \mathbb{R}^{(n-p) \times p}}, \quad \varphi_E \circ \Psi_E = \text{id}_{\mathcal{B}}. \quad \square$$

The general pattern underlying  $\varphi_E$  is revealed by writing

$$\varphi_E(\xi) = (E \exp_m(E^T \xi) + (I - EE^T)\xi) (I_p + \xi^T (I - EE^T)\xi)^{-\frac{1}{2}}, \quad \xi = \begin{bmatrix} A \\ B \end{bmatrix}.$$

Since  $(I_{p \times p} + B^T B)$  is symmetric positive definite, the inverse and the square root of the inverse are uniquely defined.

By construction, the coordinate center is

$$\varphi_E \left( \begin{bmatrix} 0 \\ 0 \end{bmatrix} \right) = E.$$

**3.1. Changing the coordinate center.** Suppose that  $\hat{U} \in \text{St}(n, p)$  is a point that we designate as the center of the coordinate chart. Let  $\hat{\mathbf{Q}} = [\hat{U} \ \hat{U}_\perp] \in \text{O}(n)$  be an arbitrary but fixed orthogonal completion. Define

$$(3.2) \quad \varphi_{\hat{U}} : T_{\hat{U}} \text{St}(n, p) \rightarrow \text{St}(n, p), \quad \xi \mapsto \varphi_{\hat{U}}(\xi) := \hat{\mathbf{Q}} \varphi_E \left( \hat{\mathbf{Q}}^T \xi \right),$$

$$(3.3) \quad \psi_{\hat{U}} : \mathcal{B}_{\hat{U}} \rightarrow T_{\hat{U}} \text{St}(n, p), \quad U \mapsto \psi_{\hat{U}}(U) := \hat{\mathbf{Q}} \psi_E \left( \hat{\mathbf{Q}}^T U \right).$$

Formally, these maps constitute a parameterization and a corresponding chart with coordinate center  $\hat{U} = \varphi_{\hat{U}}(0)$ ,  $0 = \psi_{\hat{U}}(\hat{U})$ .

In practical computations, where  $n \gg p$ , it is infeasible to actually form the completion  $\hat{U}_\perp$ . Fortunately, by standard Stiefel techniques we do not have to. Consider a tangent vector

$$\xi = \hat{\mathbf{Q}} \begin{bmatrix} A \\ B \end{bmatrix} = \hat{U} A + \hat{U}_\perp B = \hat{U} (\hat{U}^T \xi) + (I - \hat{U} \hat{U}^T) \xi.$$

A calculation validates the following  $\mathcal{O}(np^2)$  matrix formulae:

$$(3.4) \quad \varphi_{\hat{U}}(\xi) = \left( \hat{U} \exp_m(\hat{U}^T \xi) + (I - \hat{U} \hat{U}^T) \xi \right) \left( I_p + \xi^T (I - \hat{U} \hat{U}^T) \xi \right)^{-\frac{1}{2}},$$

$$(3.5) \quad \psi_{\hat{U}}(U) = \hat{U} \log_m \left( \hat{U}^T U (U^T \hat{U} \hat{U}^T U)^{-\frac{1}{2}} \right) + (I - \hat{U} \hat{U}^T) U (U^T \hat{U} \hat{U}^T U)^{-\frac{1}{2}}.$$

Since  $A = \hat{U}^T \xi \in \text{skew}(p)$ , computing the matrix exponential is efficient and stable. Rearranging terms, we get

$$(3.6) \quad \varphi_{\hat{U}}(\xi) = \left( \hat{U} (\exp_m(A) - A) + \xi \right) \left( I_p + \xi^T \xi + A^2 \right)^{-\frac{1}{2}}.$$

With the SVD  $MSR^T = \hat{U}^T U$ , the argument of the matrix logarithm that appears in  $\psi_{\hat{U}}(U)$  is the orthogonal matrix  $\hat{U}^T U (U^T \hat{U} \hat{U}^T U)^{-\frac{1}{2}} = MR^T$ . The expression reduces to

$$(3.7) \quad \psi_{\hat{U}}(U) = \hat{U} (\log_m(MR^T) - MR^T) + URS^{-1}R^T.$$

It is interesting to observe that  $MR^T \in \text{O}(p)$  is the solution to the Procrustes problem  $\min_{Q \in \text{O}(p)} \|U - \hat{U}Q\|_F$ , i.e., it is the rotation that brings  $U$  closest to  $\hat{U}$ , see [6, Section 6.4.1].

**3.2. Retraction order.** Retractions are approximations of the Riemannian exponential map. The Riemannian exponential depends on the chosen metric. Given a base point  $\hat{U} \in \text{St}(n, p)$  and an arbitrary but fixed orthogonal completion  $\hat{\mathbf{Q}} = [\hat{U} \ \hat{U}_\perp] \in O(n)$ , the Riemannian exponential on the Stiefel manifold under the one-parameter family of metrics of [8] reads

$$(3.8) \quad \begin{aligned} & \text{Exp}_{\hat{U}} : T_{\hat{U}} \text{St}(n, p) \rightarrow \text{St}(n, p), \\ & \xi = \hat{\mathbf{Q}} \begin{bmatrix} A \\ B \end{bmatrix} \mapsto \hat{\mathbf{Q}} \exp_m \left( \begin{bmatrix} 2\beta A & -B^\top \\ B & 0 \end{bmatrix} \right) \begin{bmatrix} I_p \\ 0 \end{bmatrix} \exp_m((1 - 2\beta)A), \end{aligned}$$

see [17, eq. (11)]. The canonical and the Euclidean metric correspond to  $\beta = \frac{1}{2}$  and  $\beta = 1$ , respectively. By definition, a retraction of order  $k$  coincides with the Taylor expansion of  $\xi \mapsto \text{Exp}_U(\xi)$  around  $0 \in T_U \text{St}(n, p)$  up to terms of  $k$ th order. It holds

$$\xi \mapsto \text{Exp}_U(0 + \xi) = \hat{\mathbf{Q}}E + D(\text{Exp}_U)_0[\xi] + D^2(\text{Exp}_U)_0[\xi, \xi] + \mathcal{O}(\|\xi\|^3),$$

where

$$D(\text{Exp}_U)_0[\xi] = \hat{\mathbf{Q}} \begin{bmatrix} A \\ B \end{bmatrix} = \xi, \quad D^2(\text{Exp}_U)_0[\xi, \xi] = \hat{\mathbf{Q}} \begin{bmatrix} A^2 - B^\top B \\ (2 - 2\beta)BA \end{bmatrix}.$$

The first equation means  $D(\text{Exp}_U)_0 = \text{id}|_{T_U \text{St}(n, p)}$ , which is a classical fact from Riemannian geometry. Since this is independent of the metric parameter, any retraction is a (first-order) retraction for the whole metric family. It is well known that the classical polar factor retraction from (2.1) is of second-order under the Euclidean metric.<sup>2</sup> The maps  $\varphi_{\hat{U}}$  from (3.2) share this property.

**LEMMA 3.3.** *The family of maps  $\{\varphi_{\hat{U}} \mid \hat{U} \in \text{St}(n, p)\}$  from (3.1),(3.2) is a retraction under any metric of the one-parameter family. Under the Euclidean metric, it is a retraction of second order.*

*Proof.* Using the series expressions for the matrix exponential, matrix inversion and the matrix square root, the Taylor expansion of  $t \mapsto \varphi_{\hat{U}}(t\xi)$  at  $t = 0$  in the direction  $\xi = \hat{\mathbf{Q}} \begin{bmatrix} A \\ B \end{bmatrix} \in T_{\hat{U}} \text{St}(n, p)$  is seen to be

$$\varphi_{\hat{U}}(t\xi) = \hat{\mathbf{Q}} \varphi_E \left( 0 + t \begin{bmatrix} A \\ B \end{bmatrix} \right) = \hat{\mathbf{Q}} \left( I + tA + \frac{1}{2}t^2(A^2 - B^\top B) + \mathcal{O}(t^3) \right) \begin{bmatrix} I_p \\ tB - \frac{1}{2}t^3 B B^\top B + \mathcal{O}(t^5) \end{bmatrix},$$

which shows that  $\varphi_{\hat{U}}$  matches the Riemann exponential  $\text{Exp}_{\hat{U}}$  under any  $\beta$ -metric up to terms of order one, and up to terms of order two under the Euclidean metric ( $\beta = 1$ ).

Equation (3.4) reveals smooth, even analytic dependence on the base point  $\hat{U} \in \text{St}(n, p)$ .  $\square$

**4. Preliminary experimental results.** The numerical experiments are conducted with the function implementations as listed in Appendix A.

*Accuracy.* First, we evaluate the accuracy of the polar-light retraction by quantifying its deviation from the corresponding Riemannian geodesic. To this end, we compute a pseudo-random data triple  $U_0, U_1 \in \text{St}(n, p)$ ,  $\xi \in T_{U_0} \text{St}(n, p)$  such that

$$\text{Exp}_{U_0}(\xi) = U_1, \quad \text{dist}_e(U_0, U_1) = \frac{\pi}{2},$$

<sup>2</sup>The Taylor expansion is  $R_{\hat{U}}(t\xi) = \hat{U} + t\xi + \frac{1}{2}t^2 \hat{U}(A^2 - B^\top B) + \mathcal{O}(t^3)$ .

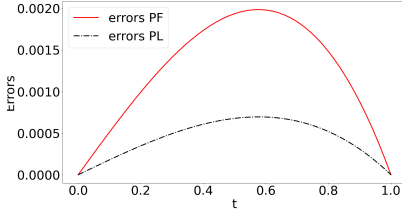
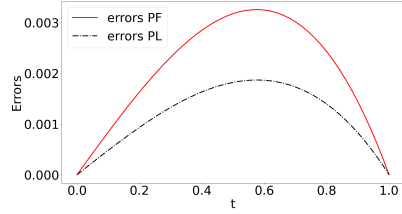
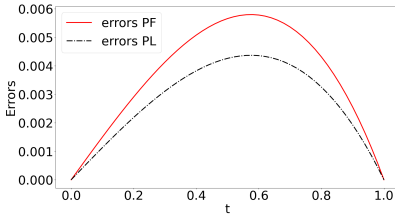
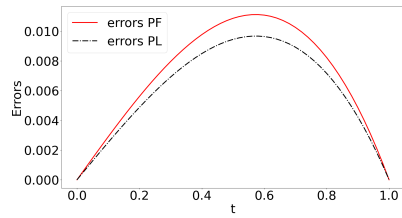
(a) for  $U_0, U_1 \in \text{St}(n, p)$ ,  $n = 1000, p = 400$ ,  $\text{dist}(U_0, U_1) = \frac{\pi}{2}$ .(b) for  $U_0, U_1 \in \text{St}(n, p)$ ,  $n = 1000, p = 200$ ,  $\text{dist}(U_0, U_1) = \frac{\pi}{2}$ .(c) for  $U_0, U_1 \in \text{St}(n, p)$ ,  $n = 1000, p = 100$ ,  $\text{dist}(U_0, U_1) = \frac{\pi}{2}$ .(d) for  $U_0, U_1 \in \text{St}(n, p)$ ,  $n = 1000, p = 50$ ,  $\text{dist}(U_0, U_1) = \frac{\pi}{2}$ .

Fig. 1: The figure shows the error  $\|\text{Exp}_{U_0}(t\xi) - R_{U_0}(t\xi_R)\|_F$  between the Riemannian geodesic connecting  $U_0$  and  $U_1 = \text{Exp}_{U_0}(t\xi)|_{t=1}$  and a retraction curve from  $U_0$  to the same point  $U_1 = R_{U_0}(t\xi_R)|_{t=1}$ . As retractions, the polar factor retraction (2.1) (PF, solid red line) and the polar-light retraction (3.6) (PL, dashed black line) are considered.

where  $\text{dist}_e$  denotes the Euclidean Stiefel metric associated with  $\beta = 1$  in (3.8). The geodesic connecting  $U_0, U_1$  is

$$\gamma_E : [0, 1] \rightarrow \text{St}(n, p), t \mapsto \text{Exp}_{U_0}(t\xi).$$

To obtain a retraction  $R_{U_0}$  connecting the same endpoints, we compute  $R_{U_0}^{-1}(U_1)$ . This yields a tangent vector  $\xi_R$  with  $R_{U_0}(\xi_R) = U_1$ . The retraction curve connecting the given endpoints is

$$\gamma_R : [0, 1] \rightarrow \text{St}(n, p), t \mapsto R_{U_0}(t\xi).$$

We discretize the unit interval  $[0, 1]$  in 51 equidistant steps  $t_k$  and compute the error between geodesic and the retraction curve in the Forbenius norm

$$\text{error} = \|\gamma_E(t_k) - \gamma_R(t_k)\|_F.$$

As retractions, we use the full polar factor retraction (PF) of (2.1) and the polar-light retraction (PL) of (3.6). Figure 1 displays the error curves for dimensions  $n = 1000$  and  $p \in \{400, 200, 100, 50\}$ . The maximal errors are listed in Table 1.

As can be seen from the figure and the table, the polar-light retraction is consistently closer to the Riemannian geodesic than the full polar factor retraction. The difference is more pronounced for larger values of  $p$ . Intuitively, this makes sense,

Table 1: Error maxima of the retraction curves considered in Figure 1

$p$	max error PF	max error PL
400	1.984e-3	6.954e-4
200	3.255e-3	1.868e-3
100	5.799e-3	4.369e-3
50	1.111e-2	9.665e-3

since the difference between the PF- and the PL-retraction is only in the treatment of the  $(p \times p)$ -block  $A$ , cf. (2.1) and (3.6). For  $A = 0$ , both maps coincide.

*Computation time.* To assess the computational effort, we create 100 pseudo-random points  $U_0, U_1 \in \text{St}(n, p)$  of dimensions  $n = 1000, p = 400$ . Then, we measure the time<sup>3</sup> it takes to perform 100 calculations of  $R_{U_0}^{-1}(U_1)$ . On the side, we also assess the identity  $R_{U_0}^{-1} \circ R_{U_0} = \text{id}_{T_{U_0} \text{St}(n, p)}$  by computing the norm  $\|R_{U_0}^{-1} \circ R_{U_0}(\xi) - \xi\|_F$  averaged over the number of runs. For the inverse of the full polar factor retraction and the inverse of the polar-light retraction, we obtain an average runtime and an average norm listed in Table 2.

By comparing (2.1) to (3.6), it is clear that the (forward) polar-light retraction is more costly to evaluate than the full polar factor retraction. Computations that do not depend on  $n$  aside, the essential difference is that the former features a term  $(UM + \xi)$ , while for the latter, the corresponding term is only  $(U + \xi)$ .

Table 2: Average computation time based on 100 inverse retraction evaluations on  $\text{St}(n, p)$ ,  $n = 1000, p = 400$ .

Retraction	average time	average $\ R_{U_0}^{-1} \circ R_{U_0}(\xi) - \xi\ _F$
inv. PF	0.1480s	2.3224e-13
inv. PL	0.1160s	1.3934e-13

**5. Conclusions and future work.** By a modification of the classical polar factor retraction on the Stiefel manifold, we provided a new Stiefel retraction that is second-order accurate under the Euclidean metric and features a closed-form inverse.

The proposed polar-light retraction incurs a higher computational cost in forward evaluation compared to the classical polar factor retraction, mainly owing to an additional  $(n \times p)$  times  $(p \times p)$  matrix-matrix product in the factor  $(U(\exp_m(A) - A) + \xi)$  in (3.7). However, its inverse can be computed more efficiently. This may be beneficial in logarithm-heavy calculations such as computing Riemannian barycenters.

We see the main benefit in having a closed-form expression for the inverse of the polar-light retraction. The formulas make it explicit how the independent parameters  $A \in \text{skew}(p)$ ,  $B \in \mathbb{R}^{(n-p) \times p}$  of a Stiefel tangent matrix  $\xi = \mathbf{Q} \begin{bmatrix} A \\ B \end{bmatrix}$  enter the calculation. Preliminary numerical experiments show that the polar-light retraction is consistently closer to the associated Stiefel geodesics than the classical polar factor retraction. *In particular, the contribution of the A-block is captured more accurately by the polar-light retraction.* (For  $A = 0$ , the polar-light retraction and the full polar factor retraction coincide.)

<sup>3</sup>Timing results are obtained with Python on a 64bit HP Z-Book with 16GB RAM and 12 CPUs of type Intel(R) Core(TM) i7-8850H CPU @ 2.60GHz.

Having a closed-form expression at hand may also be advantageous when conducting Hermite interpolation as is done in [9] for the Grassmann manifold.

There is room for computational improvements. The matrix exponential and matrix logarithm functions may be consistently replaced with their Cayley approximations

$$\exp_m(A) \approx \text{Cay}(A) = (I - \frac{1}{2}A)^{-1}(I + \frac{1}{2}A), \quad \log_m(R) \approx \text{Cay}^{-1}(R)$$

without compromising the second-order property of the retraction. Likewise, one may approximate  $(\exp_m(A) - A) \approx I + \frac{1}{2}A^2$  in  $(U(\exp_m(A) - A) + \xi)$  and adjust all other terms accordingly to get an even more efficient forward second-order retraction. Yet, when doing so, we expect that computing the inverse would fall back to solving a matrix equation similar to the full polar factor retraction.

**Appendix A. Python code.** We list the Python code that was used to conduct the numerical experiments. The code is contained in the file "Stiefel\_retractions.py" that is available at GitHub.<sup>4</sup> The implementation uses the preinstalled matrix general-purpose functions  $\exp_m$ ,  $\log_m$  and  $\text{sqrt}_m$ . Performance may be enhanced by customized implementations that take advantage of the skew-symmetric, orthogonal and symmetric structure of the input matrices, respectively.

```
#-----
import numpy as np
import scipy
from scipy import linalg

#-----
# Polar-light retraction
# PL_U0 (Xi ) = (U0exp(U0'*Xi) + (I-U0U0')*Xi
#              *(I + XiT(I-U0U0')Xi )^(-1/2)
#
# Input arguments
#      U0 : base point on St(n,p)
#      Xi : tangent vector in T_U0 St(n,p)
# Output arguments
#      U1 : PL_U0(Xi)
#-----
def Stiefel_PL_ret(U0, Xi):
#-----
    # get dimensions
    n,p = U0.shape

    A = np.dot(U0.T,Xi) # horizontal component

    expA_A = scipy.linalg.expm(A) - A
    U1      = np.dot(U0, expA_A) + Xi

    # compute matrix square root
    # first, QR of (I-U0U0^T)Xi = Xi - U0*A, only R-factor is needed
    S = np.linalg.qr(Xi-U0.dot(A), mode='r')
```

<sup>4</sup>[https://github.com/RalfZimmermannSDU/RiemannStiefelLog/tree/main/Stiefel\\_log\\_general\\_metric/SciPy](https://github.com/RalfZimmermannSDU/RiemannStiefelLog/tree/main/Stiefel_log_general_metric/SciPy)

```

S = np.eye(p) + np.dot(S.T, S)
S = scipy.linalg.sqrtm(scipy.linalg.inv(S))

# assemble U1
U1 = U1.dot(S)
return U1
#-----

#-----
# Polar-light inverse retraction
# PL_inv_U0 (U1) = (U0(logm(MR') -MR') + U1R(S^-1)R'
# where MSR' = U0'*U1 (SVD)
# Input arguments
#     U0 : base point on St(n,p)
#     U1 : end point
# Output arguments
#     Xi : tangent vector
#-----

def Stiefel_PL_inv_ret(U0, U1):
    # get dimensions
    n,p = U0.shape

    M, S, RT = scipy.linalg.svd(np.dot(U0.T,U1),\
                                full_matrices=True,\
                                compute_uv=True,\
                                overwrite_a=True)

    MRT = M.dot(RT)

    RinvSRT = np.dot( (RT.T*(1./S)), RT)

    # assemble Xi
    Xi = U0.dot((linalg.logm(MRT) - MRT)) + U1.dot(RinvSRT)
    return Xi
#-----

#-----
# Polar factor retraction
# PF_U0 (Xi ) = (U0 + Xi)(I + XiT Xi )^-1/2
#
# Input arguments
#     U0 : base point on St(n,p)
#     Xi : tangent vector in T_U0 St(n,p)
# Output arguments
#     U1 : PF_U0(Xi)
#-----

def Stiefel_PF_ret(U0, Xi):
#-----
    # get dimensions
    n,p = U0.shape

    # QR decomposition of Xi, only R-factor is needed
    S = np.linalg.qr(Xi, mode='r')
```

```

S = np.eye(p,p) + np.dot(S.transpose(), S)
# compute matrix square root
S = linalg.sqrtm(scipy.linalg.inv(S))

# assemble U1 = U0*M + Q*N
U1 = np.dot((U0+Xi),S)
return U1
#-----

#-----
# Polar factor inverse retraction
#
# Input arguments
#     U0 : base point on St(n,p)
#     U1 :     point on St(n,p)
# Output arguments
#     Xi : tangent vector in T_U0 St(n,p)
#-----
def Stiefel_PF_inv_ret(U0, U1):
#-----
    # get dimensions
    n,p = U0.shape

    M = (-1)*np.dot(U0.T,U1)

    # solve Sylvester equation MX + XM = -2*eye(p)
    X = scipy.linalg.solve_sylvester(M, M.T, (-2)*np.eye(p,p))

    Xi = U1.dot(X) - U0

    return Xi
#-----

```

## REFERENCES

- [1] P.-A. ABSIL, R. MAHONY, AND R. SEPULCHRE, *Optimization Algorithms on Matrix Manifolds*, Princeton University Press, Princeton, New Jersey, 2008, <http://press.princeton.edu/titles/8586.html>.
- [2] T. BENDOKAT AND R. ZIMMERMANN, *Efficient quasi-geodesics on the Stiefel manifold*, in Geometric Science of Information, F. Nielsen and F. Barbaresco, eds., Lecture Notes in Computer Science, Springer, 2021, pp. 763–771, [https://doi.org/10.1007/978-3-030-80209-7\\_82](https://doi.org/10.1007/978-3-030-80209-7_82).
- [3] A. EDELMAN, T. A. ARIAS, AND S. T. SMITH, *The geometry of algorithms with orthogonality constraints*, SIAM Journal on Matrix Analysis and Applications, 20 (1998), pp. 303–353, <http://dx.doi.org/10.1137/S0895479895290954>.
- [4] E. S. GAWLIK AND M. LEOK, *High-order retractions on matrix manifolds using projected polynomials*, SIAM Journal on Matrix Analysis and Applications, 39 (2018), pp. 801–828, <https://doi.org/10.1137/17M1130459>.
- [5] R. GODEMENT, *Introduction to the Theory of Lie Groups*, Universitext, Springer International Publishing, 2017.
- [6] G. H. GOLUB AND C. F. VAN LOAN, *Matrix Computations*, The John Hopkins University Press, Baltimore, 4th ed., 2013.
- [7] N. J. HIGHAM, *Functions of Matrices: Theory and Computation*, Society for Industrial and Applied Mathematics, Philadelphia, PA, USA, 2008.
- [8] K. HÜPER, I. MARKINA, AND F. SILVA LEITE, *A Lagrangian approach to extremal curves on Stiefel manifolds*, Journal of Geometrical Mechanics, 13 (2021), pp. 55–72.
- [9] R. JENSEN AND R. ZIMMERMANN, *Maximum volume coordinates for Grassmann interpo-*

- lation: *Lagrange, Hermite, and errors*, 2025, <https://arxiv.org/abs/2506.01574>, <https://arxiv.org/abs/2506.01574>.
- [10] T. KANEKO, S. FIORI, AND T. TANAKA, *Empirical arithmetic averaging over the compact Stiefel manifold*, IEEE Transactions on Signal Processing, 61 (2013), pp. 883–894, <https://doi.org/10.1109/TSP.2012.2226167>.
- [11] S. MATAIGNE, R. ZIMMERMANN, AND N. MIOLANE, *An efficient algorithm for the Riemannian logarithm on the Stiefel manifold for a family of Riemannian metrics*, SIAM Journal on Matrix Analysis and Applications, 46 (2025), pp. 879–905, <https://doi.org/10.1137/24M1647801>.
- [12] X. PENNEC, *Intrinsic statistics on Riemannian manifolds: Basic tools for geometric measurements*, Journal of Mathematical Imaging and Vision, 25 (2006), p. 127, <https://doi.org/10.1007/s10851-006-6228-4>, <https://doi.org/10.1007/s10851-006-6228-4>.
- [13] H. SATO AND K. AIHARA, *Cholesky QR-based retraction on the generalized Stiefel manifold*, Comput. Optim. Appl., 72 (2019), p. 293–308, <https://doi.org/10.1007/s10589-018-0046-7>.
- [14] M. SUTTI, *A single shooting method with approximate Frechet derivative for computing geodesics on the Stiefel manifold*, Electron. Trans. Numer. Anal., 60 (2024), pp. 501–519, [https://doi.org/10.1553/etna\\_vol60s501](https://doi.org/10.1553/etna_vol60s501).
- [15] Z. WEN AND W. YIN, *A feasible method for optimization with orthogonality constraints*, Mathematical Programming, 142 (2013), pp. 397–434, <https://doi.org/10.1007/s10107-012-0584-1>.
- [16] R. ZIMMERMANN, *A matrix-algebraic algorithm for the Riemannian logarithm on the Stiefel manifold under the canonical metric*, SIAM Journal on Matrix Analysis and Applications, 38 (2017), pp. 322–342, <https://doi.org/10.1137/16M1074485>.
- [17] R. ZIMMERMANN AND K. HÜPER, *Computing the Riemannian logarithm on the Stiefel manifold: Metrics, methods, and performance*, SIAM Journal on Matrix Analysis and Applications, 43 (2022), pp. 953–980, <https://doi.org/10.1137/21M1425426>.